A magnetoresistive self-assembled network of Gd_3Co:H nanowires

2001 J. Phys.: Condens. Matter 13 L855

(http://iopscience.iop.org/0953-8984/13/39/104)

INSTITUTE OF PHYSICS PUBLISHING JOURNAL OF PHYSICS: CONDENSED MATTER

J. Phys.: Condens. Matter **13** (2001) L855–L860 PII: S0953-8984(01)27814-X

LETTER TO THE EDITOR

A magnetoresistive self-assembled network of Gd_3Co:H nanowires

A Miniotas, R Bručas[1] and B Hjörvarsson

Materials Physics, Royal Institute of Technology, SE-100 44, Stockholm, Sweden

E-mail: bjorgvin@matphys.kth.se (B Hjörvarsson)

Received 8 August 2001
Published 13 September 2001
Online at stacks.iop.org/JPhysCM/13/L855

Abstract

In this letter we show that upon deposition of a Gd and Co mixture ($Gd_{0.985}Co_{0.015}$ and $Gd_{0.94}Co_{0.06}$) on $CaF_2(111)$ a phase separation occurs, resulting in a self-assembled network of Gd_3Co single-crystal nanowires embedded in epitaxial Gd thin film. The density of the network scales with the Co concentration. Upon exposure to hydrogen, the Gd host reaches an optically transparent semiconducting state, while Gd_3Co remains opaque and conducting. The magnetoresistance for a $Gd_{0.94}Co_{0.06}$:H thin film is increased to $\Delta\rho/\rho(12\ \mathrm{T}) = 16$ at 1.7 K as compared with $\Delta\rho/\rho(12\ \mathrm{T}) = 4$ for pure $GdH_{3-\delta}$ thin films.

Recently, investigations of rare-earth trihydrides have attracted considerable theoretical [1–3] and experimental [4–8] attention. However, the origin of the hydrogen-induced metal–insulator transition [4] is still under debate. Recently, magnetic rare-earth hydrides revealed yet another fascinating property, namely spin-dependent transport, resulting in high negative magnetoresistivity [8].

The family of magnetic rare-earth and transition metal compounds is vast and rich in possible material combinations. Intermetallic and amorphous compounds, thin films and multilayers have been intensively studied during the last three decades. These are used for a wide range of applications, e.g. as permanent magnets and in magneto-optical recording [9]. The research efforts have concentrated on 3d-rich compounds and their hydrides. Relatively little is known about 4f-rich compounds and even less about their hydrides. Only sparse data on bulk materials of these compounds exist in the literature [10]. In the case of Gd–Co alloy, a phase separation into pure Gd and Gd_3Co intermetallic compound on the Gd-rich side of the diagram is expected [11].

In this letter we show that a phase separation of Gd and Gd_3Co phases in epitaxial thin films results in a self-assembled network of Gd_3Co nanowires embedded in the Gd host. We demonstrate that these nanowires, when loaded with hydrogen, exhibit high negative magneto-resistance at low temperatures (up to 1600% at 1.7 K).

[1] Permanent address: Department of Physics, Kaunas University of Technology, LT-3031, Kaunas, Lithuania.

Thin films of Gd- and Co-doped Gd were condensed on a $CaF_2(111)$ substrate kept at 900 K under ultrahigh-vacuum (UHV) conditions. The pressure during deposition was in the 10^{-7} Pa range. Cobalt was evaporated from a Knudsen cell, Gd and Pd from an electron-beam evaporation source. The average growth rate was 0.05 nm s^{-1}. Initially, a seeding layer of 10 nm of Gd was deposited; this was followed by 400 nm of Gd–Co alloy and the sequence was finished with 200 nm of Gd. Subsequently, the film was cooled to room temperature and Pd contacts were evaporated *in situ*. The samples prepared in such a way were used for resistivity measurements. Somewhat modified sample architecture was used when growing samples for the microscopy investigations. A 10 nm Gd seeding layer was grown and 200 nm of Gd and Co were co-deposited, after which a 10 nm Nb overlayer was grown. The Nb overlayer protects the film from oxidation, still allowing one to load the sample with hydrogen up to the trihydride state, and is thereby suitable for *ex situ* microscopy investigations. The same hydrogen-loading procedure was used for all the samples. Details of the procedure and sample schematics are described elsewhere [8].

The x-ray diffraction was measured in the standard Bragg–Brentano and rocking-curve geometries with a Siemens D-5000 diffractometer. Several important conclusions followed from the analysis of the x-ray diffraction data (figure 1, table 1). First, orthorhombic (110)-oriented crystallites of intermetallic Gd_3Co compound are evidently formed in the samples containing Co. Second, the lattice parameter of Gd is not affected by the amount of Co in the film, which is consistent with the immiscibility of the constituents. A separate intermetallic phase of Gd_3Co is formed, as can be expected from the Co–Gd phase diagram [11]. Third,

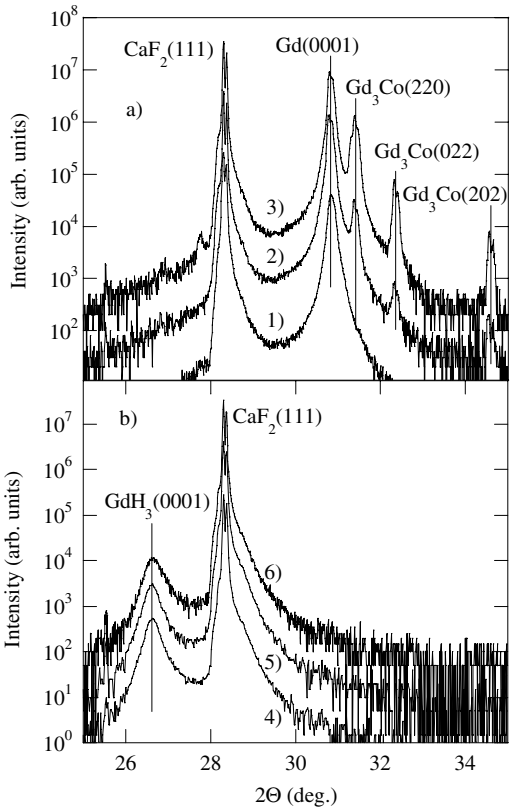

Figure 1. Θ–2Θ scans of thin films of (a) Gd (1), $Gd_{0.985}Co_{0.015}$ (2), $Gd_{0.94}Co_{0.06}$ (3) and (b) $GdH_{3-\delta}$ (4), $Gd_{0.985}Co_{0.015}$:H (5), $Gd_{0.94}Co_{0.06}$:H (6).

Table 1. Full width at half-maximum (FWHM) for the rocking curves of the thin-film peaks represented in figure 1.

Peak	0% Co	1.5% Co	6% Co
Gd(002)	0.495°	0.291°	0.261°
$Gd_3Co(220)$	—	0.277°	0.247°
$Gd_3Co(022)$	—	0.245°	0.222°
$Gd_3Co(202)$	—	0.243°	0.211°
$GdH_3(002)$	1.979°	2.547°	2.515°

the crystalline quality of the Gd and Gd_3Co parts of the film is improved as the amount of Co is increased in the film (table 1). Hence, cobalt appears to act as a surfactant for the Gd part of the film. Fourth, after hydrogen loading, the Gd_3Co phase does not exhibit reflections in the direction perpendicular to the surface of the film. This implies either a loss of long-range order in the Gd_3Co compound or a tilt of the scattering vector from the Θ–2Θ scan line. Fifth, the height of the Gd_3Co crystallites, estimated using the Scherrer formula, is of the order of 110 nm, i.e. the coherence length is comparable to the film thickness. Thus a phase separation of the constituents into Gd and Gd_3Co parts is evident from the XRD data.

To establish the topographical distribution of the Gd_3Co phase, the hydrogenated films were investigated by an optical transmission microscope. In the image of the hydrogenated $Gd_{0.985}Co_{0.015}$ thin film, figure 2(a), a network of non-transparent stripes is seen. The stripes follow $[11\bar{2}0]$ directions of Gd(0001) [12]. The optical image is not sharp in figure 2(a), because of the Fraunhofer diffraction. Hence the width of the stripes is comparable with the wavelength of light.

To obtain better spatial resolution, an atomic force microscope (AFM) was utilized. The AFM images were taken with a UHV-compatible Omicron scanning probe microscope. In the 5×5 μm AFM scan (figure 2(b)) of $Gd_{0.985}Co_{0.015}$ film a part of a stripe is seen; the whole network is displayed in figure 2(a). In an AFM image of the $Gd_{0.94}Co_{0.06}$ film (figures 2(c), 2(d)) an increase of the network density is observed. Thus, the density of the stripes increases

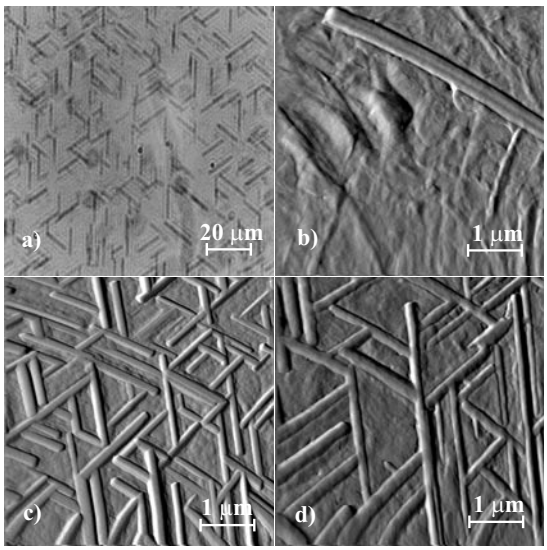

Figure 2. (a) An optical transmission microscope image of $Gd_{0.985}Co_{0.015}$:H. (b) A 5×5 μm AFM image of the same film. In (c) and (d), 5×5 μm AFM images of $Gd_{0.94}Co_{0.06}$ thin film (c) as grown and (d) hydrided are shown. The heights of the nanowires are in the range 25–50 nm.

with increase of the Co content in the film. For both samples containing Co the width of the stripes is in the 150–300 nm range a height of 25–50 nm. Since the width of the stripes is in the range of a few hundred nanometres, the term nanowires will be used. In $Gd_{0.985}Co_{0.015}$ film the nanowires are 8–12 μm long, while in the $Gd_{0.94}Co_{0.06}$ film the nanowires are shorter and range from one to several micrometres in length.

The identification of the Co-rich regions was established by an energy-dispersive x-ray (EDX) analysis on a Zeiss DSM-942 scanning electron microscope. Local EDX analysis over the nanowire revealed a high cobalt content. Thus we identify the network of the wires as consisting of Gd_3Co crystallites and the regions between these as being of Gd. This conclusion is consistent with the hydrogen-induced optical switching; i.e. Co-rich parts do not become optically transparent.

The average chemical composition and depth distribution of the films were determined by Rutherford back-scattering (RBS) and $^1H(^{15}N, \alpha\gamma)^{12}C$ nuclear resonance analysis (NRA) [13]. The ion beam analysis experiments were performed at the Tandem Accelerator in Uppsala. The RBS analysis showed that Co is present through the whole thickness of the film. The NRA revealed that the hydrogen content of the films was close to three H atoms per metal atom. Y_3Co absorbs a large quantity of hydrogen (Y_3CoH_8) [14]. Since Y and Gd are often regarded as being chemically identical and structurally substitutional, it is feasible to assume that the nanowires form Gd_3CoH_8, which is consistent with the NRA results.

The perfect rectangular shape of the as-grown Gd_3Co nanowires, the full width at half-maximum (FWHM) for the rocking curves and a coherence length of at least 110 nm suggest that the nanowires are of very good crystalline quality. The preferred orientation of the nanowires along $[11\bar{2}0]$ directions of the (0001) Gd suggest that nucleation starts at dislocations in the Gd seeding layer [15]; hence the nanowire network mimics the dislocation network.

A diffusion-limited-aggregation (DLA) model is often used to simulate thin-film growth. Directional anisotropy of the diffusion length on the surface of the film Λ_a and the average diffusion length of atoms adsorbed at the perimeter of the aggregate Λ_l determine the shape and number of the aggregates [16–18]. Both Λ_a and Λ_l represent a kinetic limitation on the film growth. At low deposition temperatures ($\Lambda_a \approx 0$, $\Lambda_l \approx 0$), amorphous Co–Gd thin films are formed [10], i.e. the thermodynamically favoured phase separation is hindered by a slow surface and bulk diffusion. At high deposition temperatures the diffusion rate is enhanced and phase separation occurs (figures 1, 2) resulting in Gd and Gd_3Co phases. The diffusion of Co along the nanowire (Λ_a) has to be extremely fast, as can be seen from the aspect ratio of the nanowires, which can be as large as 50. Co atoms diffuse a few micrometres until they are trapped at a preferential nucleation site on the surface of the wires. Furthermore, Co is immiscible with Gd and can thereby act as a surfactant for the Gd, as implied by the XRD results. The model, with Co being a surfactant for the Gd part of the film, explains the anomalously large diffusion lengths in the film and a phase separation at the micrometre scale.

The zero-field resistivity of the non-hydrogenated samples did not exhibit any anomalies, except a break in the resistivity near room temperature, corresponding to the onset of ferromagnetic ordering in Gd. Hence, the resistivity of the films with Gd_3Co nanowires is dominated by the Gd host. The resistivity of the hydrogenated samples was measured with a standard four-probe method ($I = 100$ μA) in a flowing-gas cryostat equipped with a 12 T superconducting magnet. The magnetoresistance of the films was measured with a magnetic field applied perpendicular to the plane of the sample. The RT specific resistivity decreases with increasing amount of Co, indicating the importance of the Co-doped nanowires for the conductivity. At RT the specific resistivity ρ of the $GdH_{3-\delta}$ is 8 mΩ cm, $Gd_{0.985}Co_{0.015}$:H has $\rho = 5$ mΩ cm, while the $Gd_{0.94}Co_{0.06}$:H sample has an even lower $\rho = 2.5$ mΩ cm. The samples are inhomogeneous and it is difficult to evaluate the specific resistivity for

each of the constituents of the film; hence resistivity data are presented as normalized to RT (figure 3). Above 10 K the asymptotic behaviours of the three samples are very similar. At lower temperatures the relative resistivity increases and strongly scales with Co content. In the $Gd_{0.985}Co_{0.015}$:H film the network of nanowires does not overlap (figure 2); consequently the current flows not only through the Co-doped nanowire network, but also through the Co-undoped part of the hydride. In the latter case, $\Delta\rho/\rho(280\ \mathrm{K}) = 5$ at 1.7 K as compared to almost 8 in the completely overlapping network case.

The resistivity of $GdH_{3-\delta}$ (figure 3) at 2 K exhibits a break, while in Co-doped samples this does not appear. GdH_3 orders antiferromagnetically at 1.8 K [19] and the break of the resistivity is a manifestation of ordering. Gd_3Co is a weak antiferromagnet, with $T_N = 120$ K, but there are no magnetic data available for a hydrided Gd_3Co compound. The resistivity of the $Gd_{0.94}Co_{0.06}$:H film does not show any signs of ordering down to 1.7 K, which indicates

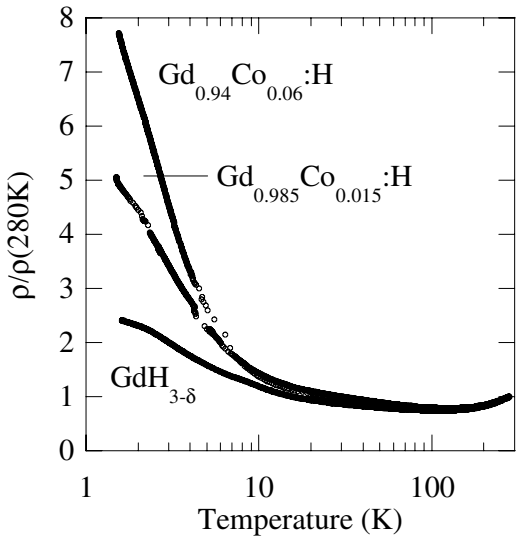

Figure 3. Zero-field resistivity of $GdH_{3-\delta}$, $Gd_{0.985}Co_{0.015}$:H and $Gd_{0.94}Co_{0.06}$:H thin films, normalized to 280 K.

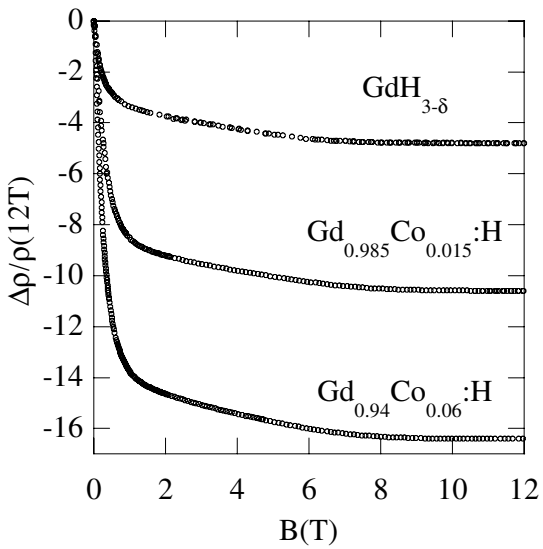

Figure 4. Magnetoresistance at 1.7 K of $GdH_{3-\delta}$, $Gd_{0.985}Co_{0.015}$:H and $Gd_{0.94}Co_{0.06}$:H thin films. The field is perpendicular to the film plane.

that the Co-rich part of the sample dominates the overall conductivity of the film.

The magnetoresistances (MR) at 1.7 K are similar for the three samples and each one shows three distinct regions, 0–1 T, 1–8 T and above 8 T (figure 4). The MR of $GdH_{3-\delta}$ is addressed in reference [8]. There, $GdH_{3-\delta}$ was shown to contain conduction-electron-enriched, magnetically ordered, dispersed volumes in the non-conducting magnetically disordered host. The low-field (<1 T) MR in $GdH_{3-\delta}$ was interpreted as occurring due to alignment of magnetically ordered volumes, hence opening a channel for spin-dependent conductivity. Above 8 T, alignment of the Gd^{3+} ions reduces the magnetic scattering in the semiconductor and opens a new spin-dependent conductivity channel. Once all Gd^{3+} ions are aligned [20], the conductivity becomes field independent. $\partial(\Delta\rho/\rho)/\partial H$ in the range 1–12 T takes values of similar magnitude for the three films. The biggest difference between the three occurs at low fields. The low-field decrease of the resistivity scales with the Co content in the film, i.e. the density of the nanowire network. The most probable scenario of the enhanced MR has to do with the presence of Co in the nanowires. Details of the underlying mechanism are not clear and require further investigation.

In summary, we show that a self-assembled network of Gd_3Co crystallites in the host of Gd can be synthesized. Upon hydride formation, a conducting network in the semiconducting environment is developed. The increase in magnetoresistance scales approximately with the Co content in the samples containing Gd_3Co compound.

We wish to acknowledge the members of the TMR Network *Switchable Metal-Hydride Films* and M Andersson and C Chacon for fruitful discussions, and NFR, TFR and the Göran Gustavsson foundation for financial support.

References

[1] Ng K K, Zhang F C, Anisimov V I and Rice T M 1997 *Phys. Rev. Lett.* **78** 1311
[2] Eder R, Pen H F and Sawatzky G A 1997 *Phys. Rev.* B **56** 10 115
[3] van Gelderen P, Bobbert P A, Kelly P J and Brocks G 2000 *Phys. Rev. Lett.* **85** 2989
[4] Huiberts J N, Griessen R, Rector J H, Wijngaarden R J, Dekker J P, de Groot D G and Koeman N J 1996 *Nature* **380** 231
[5] Huiberts J N, Rector J H, Wijngaarden R J, Jetten S, de Groot D G, Dam B, Koeman N J, Griessen R, Hjörvarsson B, Olafsson S and Cho Y S 1996 *J. Alloys Compounds* **239** 158
[6] Huiberts J N, Griessen R, Wijngaarden R J, Kremers M and Van Haesendonck C 1997 *Phys. Rev. Lett.* **79** 3724
[7] van Gogh A T M, Kooij E S and Griessen R 1999 *Phys. Rev. Lett.* **83** 4614
[8] Miniotas A, Nordblad P, Andersson M and Hjörvarsson B 2001 *Europhys. Lett.* to be published
[9] Westbrook J H and Fleischer R L (ed) 1995 *Intermetallic Compounds. Principles and Practice* vol 2 (New York: Wiley)
[10] Hansen P 1991 *Handbook of Magnetic Materials* vol 6 (Amsterdam: North-Holland)
[11] Masalski T B (ed) 1990 *Binary Alloy Phase Diagrams* (Metals Park, OH: ASM)
[12] Kerssemakers J W J, van der Molen S J, Koeman N J, Günther R and Griessen R 2000 *Nature* **406** 489
[13] Lanford W A, Trautvetter H P, Ziegler J F and Keller J 1976 *Appl. Phys. Lett.* **28** 566
[14] van Mal H H, Buschow K H J and Miedema A R 1976 *J. Less-Common Met.* **49** 473
[15] Nagengast D G, Kerssemakers J W J, van Gogh A T M, Dam B and Griessen R 1999 *Appl. Phys. Lett.* **75** 1724
[16] Witten T A and Sander L M 1983 *Phys. Rev.* B **27** 5686
[17] Hwang R Q, Schröder J, Günther C and Behm R J 1991 *Phys. Rev. Lett.* **67** 3279
[18] Röder H, Hahn E, Brune H, Bucher J P and Kern K 1993 *Nature* **366** 141
[19] Carlin R L, Chirico R D, Joung K O, Shenoy G K and Westlake R G 1980 *Phys. Lett.* A **75** 413
[20] Kietel C 1986 *Introduction to Solid State Physics* (New York: Wiley)